

Switching Off Electron Transfer Reactions in Confined Media: Reduction of $[\text{Co}(\text{dipic})_2]^-$ and $[\text{Co}(\text{edta})]^-$ by Hexacyanoferrate(II)

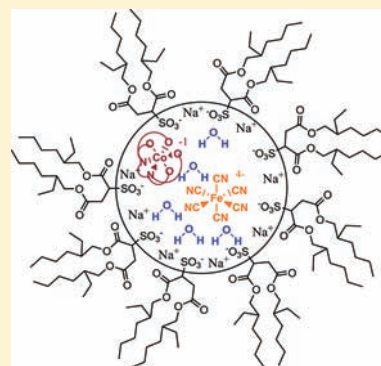
Michael D. Johnson,^{*,†} Bret B. Lorenz,[†] Patricia C. Wilkins,[†] Brant G. Lemons,[†] Bharat Baruah,[‡] Nathan Lamborn,[‡] Michelle Stahla,[‡] Pabitra B. Chatterjee,[‡] David T. Richens,[†] and Debbie C. Crans^{*,‡}

[†]Department of Chemistry and Biochemistry, New Mexico State University, Las Cruces, New Mexico 88003-8001, United States

[‡]Department of Chemistry, Colorado State University, Fort Collins, Colorado 80523-1872, United States

S Supporting Information

ABSTRACT: The kinetics of reduction of two cobalt(III) complexes with similar redox potentials by hexacyanoferrate(II) were investigated in water and in reverse micelle (RM) microemulsions. The RMs were composed of water, surfactant [(sodium(bis-(2-ethylhexyl)sulfosuccinate)), NaAOT], and isooctane. Compared to the reaction in water, the reduction rates of (ethylenediaminetetraacetato)cobaltate(III) by hexacyanoferrate(II) were dramatically suppressed in RM microemulsions whereas a slight rate increase was observed for reduction of bis-(2,6-dipicolinato)cobaltate(III). For example, the ferrocyanide reduction of $[\text{Co}(\text{dipic})_2]^-$ increased from $55 \text{ M}^{-1} \text{ s}^{-1}$ in aqueous media to $85 \text{ M}^{-1} \text{ s}^{-1}$ in a $w_o = 20$ RM. The one-dimensional (1-D) and two-dimensional (2-D) ^1H NMR and FT-IR studies are consistent with the reduction rate constants of these two complexes being affected by their location within the RM. Since reduction of $[\text{Co}(\text{edta})]^-$ is switched off, in contrast to $[\text{Co}(\text{dipic})_2]^-$, these observations are attributed to the penetration of the $[\text{Co}(\text{edta})]^-$ into the interfacial region of the RM whereas $[\text{Co}(\text{dipic})_2]^-$ is in a region highly accessible to the water pool and thus hexacyanoferrate(II). These results demonstrated that compartmentalization completely turns off a redox reaction in a dynamic microemulsion system by either reactant separation or alteration of the redox potentials of the reactants.



INTRODUCTION

Reagent confinement and solvation are factors of critical importance in directing electron transfer reactions of metal complexes.^{1,2} Studying such reactions in nonconventional media such as reverse micelles (RMs) provides an opportunity to obtain fundamental information on how reaction dynamics are impacted by local environment and reactant confinement. RMs are a ternary system composed of an organic solvent containing surfactant droplets that contain a confined water pool. The nature of the microemulsions formed by RMs and its water pool has been extensively studied.^{3–5} Specifically, the properties of the water in nanosized water pools has been found to differ from that of bulk water with respect to polarity, H-bonding, microfluidity, pH, and viscosity.^{3–5} However, the physical parameters of the water pool vary as the size of the water pool and core water decrease compared to the interfacial water.^{3–5} Although little is known about the local environment (location) of metal complexes contained within the microemulsions, the properties of such metal complexes are undoubtedly modified as the environment changes.⁶ Studies probing how confinement affects reactivity are important for potential applications. In this study we demonstrate that even in a dynamic reverse micellar system, reactions can be turned off as a function of changes in reactant environment.

Kinetic studies⁷ can serve as a sensitive tool for investigating the impact of confinement on reactions particularly when the kinetic data are combined with spectroscopic studies characterizing

the system and providing information regarding the location of the complexes.⁸ Studies such as these are particularly relevant for reactions that occur in the vicinity of a lipid interface^{4,9} because the properties of compounds are likely to be impacted by the interface. For example, fundamental information on how the reactivity of $[\text{Co}(\text{dipic})_2]^-$ changes when interacting with interfaces may be relevant to its ability to lower hyperlipidemia in diabetic Wistar rats.¹⁰ In contrast, other metal complexes, such as $[\text{VO}_2(\text{dipic})]^-$, lower both hyperlipidemia and hyperglycemia.¹¹ Since the insulin enhancing action of all of these complexes undoubtedly involves both hydrolytic and redox chemistry,¹² understanding the effects of confinement on metal complex reactivity is important.^{13–19}

An illustration of the three primary regions within a spherical RM system consisting of water and NaAOT in isooctane is shown in Figure 1: the water pool, the aqueous interface, and the hydrophobic interface region.²⁰ These regions provide very different types of environment for a solute. Metal complexes can occupy any of these three regions or span the boundary between adjacent regions. Depending on the location of metal complexes, significant changes in their chemical properties are likely to be observed which, combined with their “accessibility” for reaction with a component located in the same or adjacent phase, can dramatically alter chemical reactivity. Importantly for

Received: June 10, 2011

Published: February 14, 2012

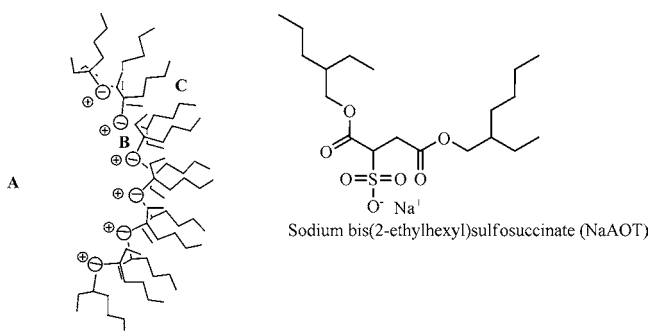


Figure 1. Structure of NaAOT and model of a RM section with possible loci for complexes labeled as water pool (A), at the interface (B), or penetrating the interface (C).

studies probing reactions, RMs are not static spheres, and their contents can mix rapidly via the formation of transient systems in which the contents of RMs are mixed or exchanged.^{20,21} This mixing or exchange rate constant is 10^6 – 10^8 $M^{-1} s^{-1}$ and is independent of the nature of the solute.^{20–25} Kinetic models in RMs have previously been described in detail and generally consider the nature of the confined water pools therein as well as interfacial effects.²²

Confined media effects on photoinduced electron transfer reactions have invoked the importance of solvent reorganization.¹ In 2005, Chakraborty observed that the photoinduced bimolecular electron transfer between different coumarin dyes and *N,N*-dimethylaniline was a factor of 3 slower in RMs than in *n*-heptane.²⁶ This outcome was attributed to either different diffusion rates in the inhomogeneous AOT system or to different accessibility of the acceptor molecules to the donor molecules induced by RM steric restrictions. More recently Dutta-Choudhury and Pal reinvestigated the photoinduced electron transfer between coumarins and amines in RMs to determine the effects of differential partitioning of quenchers; in particular, they examined the location of probes and reactant diffusion rates on the reaction rates.^{27,28} They concluded that reactant diffusion does not play a role in the quenching kinetics in RMs because rotational relaxation times and diffusion parameters do not correlate with the quenching rates. At high driving forces, inverse Marcus behavior was observed in the aqueous phase of the RM systems and was attributed to solvent reorganization energies dominating the activation process.

Studies with redox partners that adopt outer-sphere reaction pathways are particularly informative when exploring the effects of confinement on electron transfer reactions. The two oxidants used for this study; (ethylenediaminetetraacetato)cobaltate(III), $[Co(edta)]^-$, and bis(2,6-dipicolinato)cobaltate(III), $[Co(dipic)_2]^-$, Figure 2, are both structurally and spectroscopically characterized^{29–31} and well established as outer-sphere reagents suitable for Marcus theory analysis.^{32–39}

Hexacyanoferrate(II) was selected as the reductant because it is structurally well-defined in both oxidation states, well characterized as undergoing outer-sphere electron transfer reactions.^{40,41} Furthermore, its redox properties in RMs have been previously studied.^{42,43} The outer-sphere nature of the $[Co(edta)]^-$ / $[Fe(CN)_6]^{4-}$ redox process is well established³⁴ and is likely to be operative for $[Co(dipic)_2]^-$.³²

The reactions of $[Co(edta)]^-$ and $[Co(dipic)_2]^-$ with hexacyanoferrate(II) offer excellent probes to study how aqueous outer-sphere electron transfer reactions are impacted by the confined water pool within RMs. To complement the kinetic studies, we have carried out one-dimensional (1-D) and

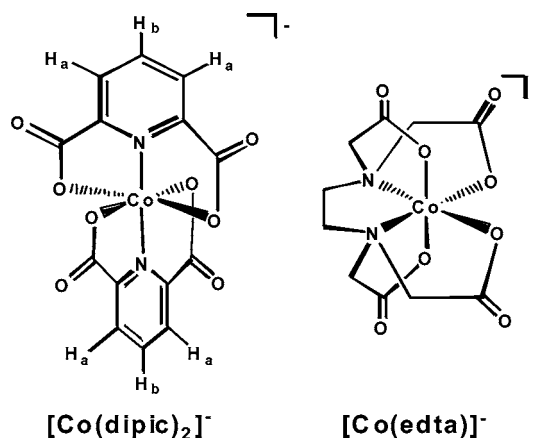


Figure 2. Structures of the cobalt(III) complexes used in this study.

two-dimensional (2-D) 1H NMR and FT-IR measurements aimed at describing the environment and location of the cobalt(III) oxidants. The two-pronged approach used in this study is important to understand the observation that $[Co(edta)]^-$ is rendered redox inactive in the RM environment and to test the hypothesis that the observed “switch off” of the reaction is due to either the reactant location or the “ionic atmosphere” encountered by the reactants within the RM.

EXPERIMENTAL SECTION

Materials. Reagent grade chemicals used in the syntheses of the cobalt complexes and in RM preparations were obtained from Aldrich and used as received unless otherwise specified. Sodium hexacyanoferrate(II) was purchased from Fisher Scientific and used without purification. A Barnsted Epure system supplied the doubly distilled, deionized (<18 $M\Omega/cm^2$) water used in all experiments. The surfactant, sodium bis-(2-ethylhexyl)sulfosuccinate (Na-AOT, 99%), used in RM preparations, was obtained from Sigma-Aldrich and purified as described previously.⁴⁴ 1H NMR spectroscopy was used to confirm Na-AOT purity.⁴⁴ Isooctane (99%) used in micro emulsion preparations was purchased from Aldrich and used as received. Hydrochloric acid was obtained from Fisher Scientific and was used without further purification. D_2O and C_6D_{12} were obtained from Cambridge Isotope Laboratories Inc.

Synthesis of Cobalt Complexes. Potassium bis(2,6-dipicolinato)cobaltate(III), $K[Co(dipic)_2]$, and potassium (ethylenediaminetetraacetato)cobaltate(III), $K[Co(edta)]$, were synthesized according to published procedures.^{10,45} Elemental analyses, UV–vis, and 1H NMR spectroscopy were used to determine product composition and purity.

Preparation of RMs. Purified Na-AOT was dissolved in isooctane at ambient temperature to make stock solutions of the surfactant. These were 0.50 M for the NMR experiments and 0.20 M for the kinetic experiments. Aqueous stock solutions of the cobalt complexes were prepared as described below. Aliquots of the aqueous solutions of the cobalt complexes were mixed with specific volumes of the Na-AOT/isooctane to prepare RMs with w_o values from 6 to 20. The w_o value is defined as the $[H_2O]/[AOT]$ ratio within the RM. Mixing of the ternary component systems was performed by sonication for 2–3 min or until separation of phases was no longer observed. Spectral and kinetic measurements were made immediately after preparation of RMs.

Kinetic Experiments. Reaction rates for the hexacyanoferrate(II) reduction of the two cobalt(III) complexes were measured using an OLIS RSM1000 stopped-flow mixing system. The reactions were monitored at 420 nm, the absorption maximum for hexacyanoferrate(III), as the absorbances for the cobalt(III) complexes were generally small under the conditions of the kinetic studies and gave less precise data. Where possible however, both loss of oxidant and appearance of

hexacyanoferrate(III) were measured and compared to confirm rate agreement. All solutions were purged with argon for a minimum of 10 min prior to mixing. The removal of dissolved oxygen was found to be important because when present in the RM systems, it caused irreproducible results. Pseudo first order conditions were used, with excess hexacyanoferrate(II) (range 0.005–0.03 M) over cobalt(III) ($\sim 5 \times 10^{-4}$ M), and the absorbance changes (average of 3–5 runs) were fitted using the OLIS data reduction software to yield the observed rate constants. Higher concentrations of hexacyanoferrate(II) did not allow formation of RMs. For the studies with $[\text{Co}(\text{dipic})_2]^-$ the solutions contained 0.5 mM dipicolinate to both buffer the reaction pH (3.0) and maintain complexation of the cobalt(II) product. Studies with $[\text{Co}(\text{dipic})_2]^-$ using 0.5 mM KHP as the buffer (no free dipicolinate) were also carried out and found to have identical electron transfer rates. This indicates that $[\text{Co}(\text{dipic})_2]^-$ remains intact within the RM and that there are no general buffer effects. The temperature was controlled to within 0.1 °C using a constant temperature bath.

Sample Preparation for ^1H NMR Spectroscopy. Aqueous solutions of each cobalt complex were adjusted to an appropriate pH for use as stock solutions for NMR analyses. The following concentrations and pH solutions were used for the 1-D NMR experiments: 33 mM $[\text{Co}(\text{dipic})_2]^-$ at pH 6.7 and 60 mM $[\text{Co}(\text{edta})]^-$ at pH 5.8. No buffers were used. RMs ranging in sizes from $w_o = 6$ to 20 were prepared using the cobalt compound stock solutions with 0.5 M Na-AOT in isoctane. Final concentrations of cobalt complexes in the RMs were from 3 mM to 11 mM. Aqueous stock solutions used as controls and RMs were prepared immediately before acquisition of NMR spectra.

^1H NMR Spectroscopy: Data Acquisition and Analysis. ^1H NMR spectra of the cobalt(III) complexes in RMs and aqueous solutions were obtained on samples placed in standard 5 mm Wilmad NMR tubes. The data were recorded at ambient temperature with 400 MHz (CSU) and 600 MHz (Pacific Northwest National Laboratory) Varian INOVA spectrometers. Routine parameters were used for the 1-D ^1H data acquisition. ^1H chemical shifts were referenced against tetramethylsilane (TMS) placed in a coaxial capillary with $\text{C}_6\text{D}_{12}/\text{TMS}$ for all samples. Linewidth calculations were performed using the Origin 7.0 curve fitting software.

^1H - ^1H -NOESY (Proton–Proton 2-D Nuclear Overhauser Enhancement Correlation Spectroscopy) NMR experiments were performed using the supplied Varian pulse sequence as reported previously.⁴⁶ Aqueous solutions of complexes were run in D_2O , to provide a lock signal, but for studies in RMs, H_2O and not D_2O was used in these samples.

Sample Preparation for FT-IR Spectroscopy. Aqueous solutions of the two cobalt(III) complexes (in mM) were prepared by using 5% HOD in H_2O and pure deionized-water. A series of stock solutions of each complex were prepared to yield a constant overall Co(III) concentration in the RM (0.70 mM for $\text{K}[\text{Co}(\text{dipic})_2]$ and 1.27 mM for $\text{K}[\text{Co}(\text{edta})]$). The RMs were assembled using 0.2 M NaAOT with w_o values of 6 and 10.

FT-IR Spectroscopy: Data Acquisition and Analysis. IR spectra were collected with a Nicolet, Magna 760 FT-IR spectrophotometer. Individual spectra represent averages of 128 scans with 1.0 cm^{-1} resolution. RM samples were introduced by using an IR microvolume cuvette with BaF_2 windows (2 mm thick) and a Teflon spacer with thickness of 50 μm . Spectra were obtained from samples in both 5% HOD in H_2O and in pure deionized-water allowing the exploration of both the OD and the OH stretching regions. To measure the spectrum from the RMs that arises only from the OD stretching signal, spectra collected with deionized-water as the polar solvent were subtracted from spectra collected using 5% HOD in H_2O . All FT-IR experiments were conducted at a constant temperature of 25 °C.

RESULTS

RM Environment Effects on the Reduction Kinetics of the Co(III) Complexes. Under pseudo first order conditions the absorbance versus time plots in aqueous media for the appearance of hexacyanoferrate(III) (420 nm) or, when possible,

the disappearance of aqueous $[\text{Co}(\text{edta})]^-$ (538 nm) and $[\text{Co}(\text{dipic})_2]^-$ (511 nm) fitted well to a single exponential. This established the first order dependence with respect to both oxidants and allowed determination of pseudo first order rate constants. Linear plots of these rate constants versus the concentration of hexacyanoferrate(II), see, for example, Figure 3, gave the second order rate constants, k_1 , listed in Table 1.

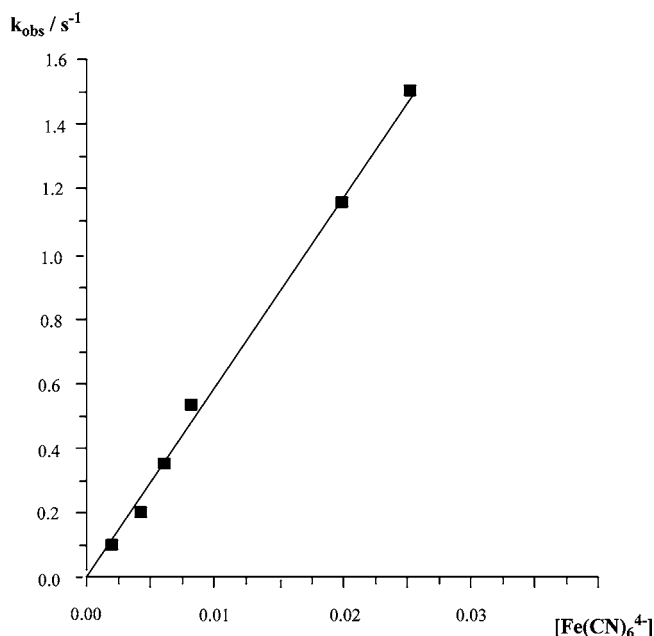


Figure 3. Typical plot of observed aqueous pseudo first-order rate constants versus hexacyanoferrate(II) concentration for the reduction of $[\text{Co}(\text{dipic})_2]^-$.

Table 1. Bimolecular Rate Constants, k_1 , for the Reduction of $[\text{Co}(\text{dipic})_2]^-$ and $[\text{Co}(\text{edta})]^-$ by Hexacyanoferrate(II) in Aqueous Solution and as a Function of w_o of the RM

oxidant	conditions*	$k_1 / \text{M}^{-1} \text{ s}^{-1}$
$[\text{Co}(\text{dipic})_2]^-$	aqueous	55 ± 7
	$w_o = 20$	85 ± 5
	$w_o = 15$	80 ± 15
	$w_o = 10$	80 ± 11
	$w_o = 7$	65 ± 7
$[\text{Co}(\text{edta})]^-$	aqueous	0.34 ± 0.03
	$w_o = 12$	no detectable reaction
	$w_o = 11$	no detectable reaction
	$w_o = 7$	no detectable reaction
	$w_o = 6$	no detectable reaction

*0.2 M NaAOT, $[\text{Co}(\text{III})] = \sim 0.5 \text{ mM}$, $[\text{Fe}(\text{CN})_6^{4-}] = 5\text{--}30 \text{ mM}$ at $T = 25.0 \text{ }^\circ\text{C}$. For $[\text{Co}(\text{dipic})_2]^-$ the runs were monitored at pH 3 with excess dipicolinate or at pH = 3 buffered with 0.5 mM potassium hydrogen phosphate in the absence of excess dipicolinate.

The value of k_1 in aqueous media obtained for the reduction of $[\text{Co}(\text{edta})]^-$ by hexacyanoferrate(II), Table 1, agrees well with the value ($0.21 \text{ M}^{-1} \text{ s}^{-1}$) reported by Haim et al.³⁴

In RMs, the UV–visible spectra of the reactants were found to be invariant in both peak position as well as extinction coefficient under the conditions of the kinetic studies when compared with the values in aqueous media (see Supporting Information, Figure S1). For $[\text{Co}(\text{edta})]^-$ the λ_{max} of 538 nm,

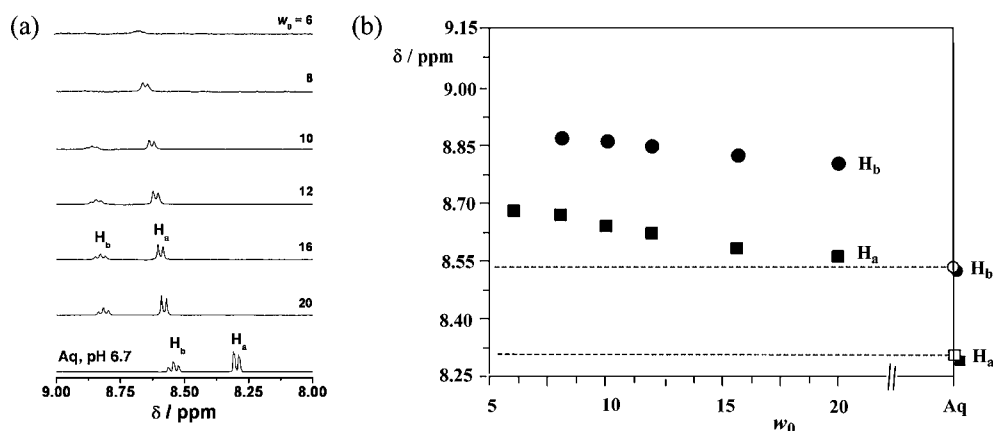


Figure 4. (a) 400 MHz ^1H NMR spectra of 33 mM $[\text{Co}(\text{dipic})_2]^-$, conditions: pH 6.7, 0.5 M AOT/isooctane RMs, $w_0 = 6, 8, 10, 12, 16,$ and 20; (b) plot of chemical shift versus w_0 (the dotted lines represent the chemical shifts in aqueous media).

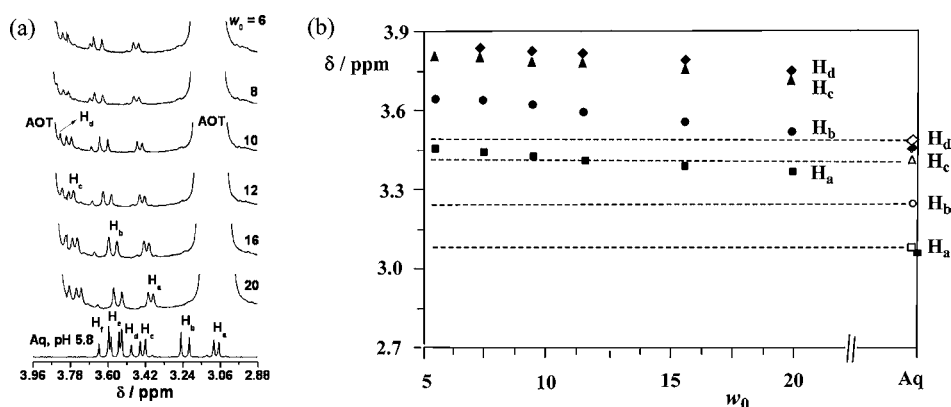


Figure 5. (a) 400 MHz ^1H NMR spectra of 60 mM $[\text{Co}(\text{edta})]^-$, conditions: pH 5.8, 0.5 M AOT/isooctane RMs, $w_0 = 6, 8, 10, 12, 16$ and 20); (b) plot of chemical shift versus w_0 (the dotted lines represent the chemical shifts in aqueous media).

in both aqueous and in RMs, is consistent with retention of the hexadentate structure with no dissociation of a carboxylate arm.⁴⁷ Pseudo first order conditions were again employed as for the aqueous studies. Identical rate constants, within experimental error, were obtained when monitoring either the appearance of hexacyanoferrate(III) at 420 nm or the disappearance of cobalt(III) oxidant. Second order rate constants are listed in Table 1 for each oxidant as a function of the w_0 value of the RM. With $[\text{Co}(\text{dipic})_2]^-$, the rate constants show an increase upon changing from aqueous media to RMs and are essentially independent of the size of the RM between $w_0 = 10$ and 20. At $w_0 = 7$ a decrease of the observed rate constant occurs. In contrast, no observable reduction of $[\text{Co}(\text{edta})]^-$ by hexacyanoferrate(II) is seen following the introduction of the complex into the RM at w_0 values of 6, 7, 11, and 12. Increasing the concentration of hexacyanoferrate(II) by 20-fold over cobalt(III) as well as monitoring over longer time periods (up to one week) failed to show evidence of any reduction of the $[\text{Co}(\text{edta})]^-$ complex within the RM.

1-D ^1H NMR of the Cobalt(III) Complexes in AOT/Isooctane RMs. $[\text{Co}(\text{dipic})_2]^-$. ^1H NMR spectra obtained from aqueous solution and in RMs (0.5 M Na-AOT in isooctane) with sizes ranging from $w_0 = 6, 8, 10, 12, 16,$ and 18 are shown in Figure 4. The triplet centered at 8.54 ppm is assigned to the proton para to the nitrogen atom (H_b) and the doublet centered at 8.30 ppm assigned to the neighboring H_a protons of the coordinated dipicolinate. Placement of $[\text{Co}(\text{dipic})_2]^-$ in the smallest RMs causes a dramatic downfield shift

(up to 0.28–0.37 ppm) in both dipicolinic proton signals (Figure 4b) along with a concomitant increase in line-broadening (Figure 4a). Line-broadening and downfield shifts are more pronounced as w_0 decreases and for H_b at $w_0 = 4$ the signal is broadened into the baseline. The H_a proton continues to broaden as the water pool size decreases, but its signal remains observable even at $w_0 = 4$.

$[\text{Co}(\text{edta})]^-$. ^1H NMR spectra obtained from both aqueous solution and in RMs with sizes ranging from $w_0 = 6, 8, 10, 12, 16, 20$ are shown in Figure 5. In Figure 5a, the ^1H signals from 3.08 to 3.62 ppm, corresponding to the various edta protons, show significant downfield shifts in the RMs compared to the values in aqueous solution. The chemical shift differences are ~ 0.15 ppm for the $-\text{NCH}_2\text{CH}_2\text{N}-$ protons and ~ 0.19 ppm for the furthest upfield CH_2 -proton adjacent to the carboxylate groups. This difference in chemical shifts is large even for the largest RM ($w_0 = 20$). Further small downfield shifts are seen as the RM gets smaller. In contrast to the spectra of $[\text{Co}(\text{dipic})_2]^-$ no linebroadening is seen in any of the resonances for $[\text{Co}(\text{edta})]^-$ even at the lowest w_0 values.

2-D ^1H NMR Studies of the Cobalt(III) Complexes in AOT/Isooctane RMs. 2-D ^1H - ^1H NOESY NMR experiments were undertaken to support the interpretation of the 1-D NMR studies regarding the location of the of $[\text{Co}(\text{dipic})_2]^-$ and $[\text{Co}(\text{edta})]^-$ complexes. However, the combination of low solubility of one of the complexes and peak overlap limited the results obtained.

$[\text{Co}(\text{dipic})_2]^-$. Here the low solubility of this complex in the water pool of the RM even at the highest w_0 value of

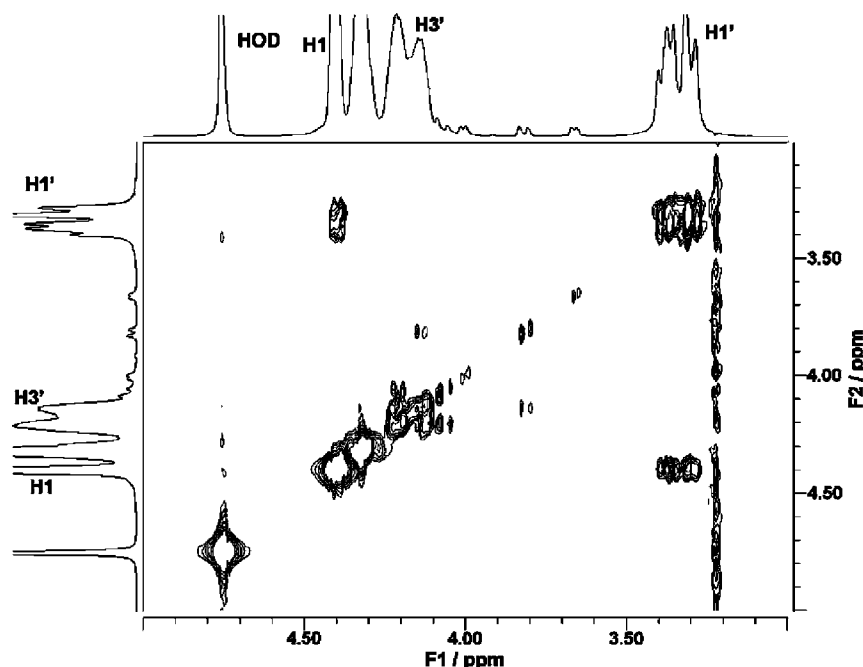


Figure 6. 2-D ^1H - ^1H NOESY NMR spectrum of 75 mM $\text{K}[\text{Co}(\text{edta})]$ in 1 M AOT/isooctane/ D_2O /pH 5.82/ $w_0 = 16$.

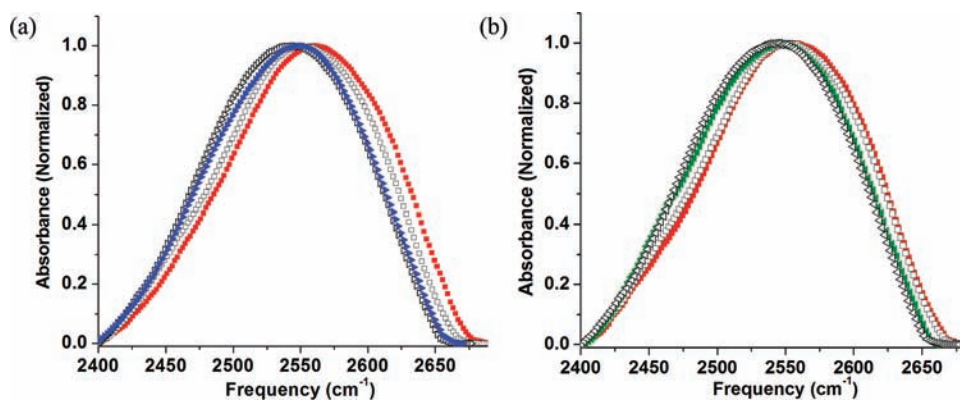


Figure 7. Normalized background subtracted FT-IR absorption spectra of the OD stretch of 5% HOD in H_2O in 0.2 M AOT RMs in the presence/absence of the cobalt(III) complexes; (a) 0.70 mM $\text{K}[\text{Co}(\text{dipic})_2]$ (squares, $w_0 = 6$; triangles, $w_0 = 10$). (b) 1.27 mM $\text{K}[\text{Co}(\text{edta})]$ (squares, $w_0 = 6$; triangles, $w_0 = 10$). Filled color symbols represent spectra in the presence of the cobalt(III) complex; open symbols reflect spectra obtained in the absence of the cobalt(III) complex.

20 prevented the observation of any 2-D NMR spectra with acceptable resolution.

$[\text{Co}(\text{edta})]^-$. The higher solubility of $[\text{Co}(\text{edta})]^-$ allowed the extraction of NOESY data at w_0 values as low as 16. Figure 6 showed evidence of a weak NOE from edta protons at 3.8 ppm and 4.08 ppm with signals for AOT in the 4.13–4.2 ppm range consistent with the $[\text{Co}(\text{edta})]^-$ complex being located near to the $\text{H}3'$ protons of the AOT and thus penetrated into the lipid interface. However the presence of overlapping shifted edta protons in the same region as the AOT protons makes for some caution in the assignment. The more intense NOESY cross peaks visible at 3.3 ppm and 4.4 ppm are assigned to AOT-AOT interactions.

FT-IR Studies of the Cobalt(III) Complexes in AOT/Isooctane RMs. FT-IR experiments were carried out to measure the OD stretch in a dilute solution of D_2O in H_2O (2.5%). These studies investigate how the two cobalt(III) complexes impact the water pool. Both of these complexes are substitution inert so dissociation, or partial dissociation, of the coordinated

ligands does not occur during the time frame of our experiments. Figure 7a,b displays the OD stretching vibration so obtained from $w_0 = 6$ and 10 AOT RMs in the presence and absence of the two complexes. In the presence of $[\text{Co}(\text{dipic})_2]^-$ the OD stretching vibration is blue-shifted by 8 and 6 cm^{-1} in the $w_0 = 6$ and 10 RMs, respectively, from the position of the vibration in the absence of the complex, Figure 7a.

When the same experiment is carried out with $[\text{Co}(\text{edta})]^-$ the corresponding blue shift in the $w_0 = 6$ and 10 RMs in the presence of the complex is much smaller (2 and 1 cm^{-1} respectively), well within the error limits of the experiment, Figure 7b. This result demonstrates that the presence of $[\text{Co}(\text{edta})]^-$ does not significantly impact the H-bonding or other water properties in the micellar water pool.

DISCUSSION

In this work our objective was to investigate how confined environments impact chemical reactions and to determine the role of location and partitioning on the reactivity of solutes.

The present study has probed the well characterized outer-sphere aqueous reduction of $[\text{Co}(\text{dipic})_2]^-$ ^{32,35} and $[\text{Co}(\text{edta})]^-$ ^{37–39,47b} by hexacyanoferrate(II)³⁴ and how they are impacted in a RM environment. Since outer-sphere electron transfer processes between transition metal complexes require direct collision of the solvated first coordination spheres, we are interested in how a RM environment and potential compartmentalization might impact these parameters. It is reasonable to assume that the redox reactions in the RMs will also occur via an outer-sphere process since the UV–visible parameters and ¹H NMR spectral features for the reactants within the RM are not changed from those observed in aqueous media, that is, the first coordination sphere for each of the species is unaltered. However when confined within the RM, we find vastly differing behavior of the two cobalt(III) complexes toward reduction by hexacyanoferrate(II). Reduction of $[\text{Co}(\text{edta})]^-$ by hexacyanoferrate(II) is completely suppressed (switched off) in the RM whereas the $[\text{Co}(\text{dipic})_2]^-$ reduction is modestly accelerated, compared to reaction in bulk water. Since the highly negatively charged reductant, $[\text{Fe}(\text{CN})_6]^{4-}$, is likely to reside within the confined water pool (region A, Figure 1)^{20–22} the observed difference must be attributed to the location/environment experienced by the two cobalt(III) complexes within the RM. For the $[\text{Co}(\text{edta})]^-$ oxidant, the suppression of the reaction is readily explained by compartmentalization of the reagents because of deep penetration of the cobalt(III) complex into the interfacial region of the RM, region C in Figure 1. Separation of the redox pair via compartmentalization will prevent collisions and thereby inhibit electron transfer.⁴⁸ In the case of $[\text{Co}(\text{dipic})_2]^-$ the reaction with $[\text{Fe}(\text{CN})_6]^{4-}$ is sustained in the RM implying that the complex resides either within or in a region highly accessible to the water pool.

To provide additional support for these ideas based upon the kinetic data, both NMR and high resolution differential FT-IR spectroscopic studies were carried out in an attempt to obtain evidence for different locations of the two Co(III) complexes within the RM environment. The 1-D ¹H NMR data, Figure 4, are consistent with the $[\text{Co}(\text{dipic})_2]^-$ complex residing in the RM water pool and thus available to sustain the redox reaction. We favor this interpretation because the ¹H NMR linewidths increase significantly as w_o decreases implying significantly different environments as the distance between the water core and the interface decrease. As seen in Figure 4a, the signals for both sets of dipic protons are broadened to such an extent that one of the signals disappears into the baseline at $w_o = 6$. Increased linebroadening is generally observed for decreased relaxation times or changes in dynamic processes.⁴⁹ Since no suitable dynamic processes exist in this system, the observed linebroadening is attributed to increased relaxation times and tumbling times of the molecule.⁵⁰ This supports $[\text{Co}(\text{dipic})_2]^-$ residing in the RM water pool. The combination of charge, geometry, and size of this complex³³ might be factors preventing penetration into the interfacial region of the RM. In contrast, no linebroadening was observed for the ¹H NMR signals of $[\text{Co}(\text{edta})]^-$ at any of the w_o values studied (20–6), Figure 5a. Therefore, $[\text{Co}(\text{edta})]^-$ must reside in a location in the RM where changes in w_o size and distance from core water to interface does not affect its environment or alternatively that corresponding effects cancel each other in all the systems examined. On the basis of these observations, a likely location for $[\text{Co}(\text{edta})]^-$ is away from the water pool and somewhat penetrated into the interface. Since the rate of reduction with hexacyanoferrate(II) is completely suppressed and independent

of w_o value (range 6–12) within the RM these results are consistent with $[\text{Co}(\text{edta})]^-$ being located deeper within the interfacial region than $[\text{Co}(\text{dipic})_2]^-$.

To probe these ideas further, 2-D ¹H NOESY NMR studies were also carried on both cobalt(III) complexes within a $w_o = 16$ RM. No evidence for NOE cross peaks between $[\text{Co}(\text{dipic})_2]^-$ with AOT was observed although the poor quality of spectra as a result of the low solubility of the Co(III) complex may be a contributing factor. However the corresponding spectrum in the presence of $[\text{Co}(\text{edta})]^-$ exhibited features consistent with the $[\text{Co}(\text{edta})]^-$ complex penetrating the lipid interface. The 2-D ¹H NMR spectrum, Figure 6, shows the presence of a NOE cross signal in the region of the H3' proton of the AOT surfactant and the H_b proton of the edta. However caution is also needed in the interpretation here since the broad H3' signal overlaps with some of the shifted protons of $[\text{Co}(\text{edta})]^-$ such that the observed cross peaks could also be due to intramolecular NOEs within the $[\text{Co}(\text{edta})]^-$ complex itself. In conclusion, the 2-D NMR data are consistent with the conclusion made based on the 1-D NMR data. However, since these results do not unequivocally rule out penetration of the $[\text{Co}(\text{edta})]^-$ as proposed as an explanation for the differing redox behavior, we explored FT-infrared spectroscopy as an alternative method to provide further evidence for the location of the two Co(III) complexes.

FT-infrared (IR) spectroscopy can provide information on the interaction of the two cobalt(III) complexes by obtaining information on the local structure of the water with the confined water pool.^{5,51,52} Measuring how the solute impacts the H-bonding in the water pool because of the sensitivity of the OH stretching frequency to molecular environments complements the NMR studies. In pure water, several intra- and intermolecular H-bonded interactions contribute to the line width and position of the OH stretching absorption, and some of these effects change in the small water pools confined within AOT/isooctane RMs.^{5,51–53} By subtracting spectra obtained from pure deionized water from those obtained in 2.5% D₂O in H₂O solution we can utilize the OD stretching mode of HOD to explore the nature of the intramolecular water in the various RM samples (Table 2).

Table 2. Normalized Background Subtracted FT-IR Data for the OD Stretch of 5% HOD in H₂O in 0.2 M AOT RMs in the Presence/Absence of the Cobalt(III) Complexes; 0.70 mM K[Co(dipic)₂]; 1.27 mM K[Co(edta)]

Cobalt(III) complex	w_o	$\nu(\text{OD})/\text{cm}^{-1}$	$\nu(\text{probe})(\text{OD}) - \nu(\text{no probe})(\text{OD})/\text{cm}^{-1}$
no probe	6	2552	
	10	2543	
K[Co(dipic) ₂]	6	2560	8
	10	2549	6
K[Co(edta)]	6	2554	2
	10	2544	1

Figure 7 shows a significant blue shift of the OD stretch when $[\text{Co}(\text{dipic})_2]^-$ is present in the RM. The blue shift can be interpreted as an overall weakening of the water H(D)-bond network consistent with solute interaction. Furthermore the disruption would be expected to be larger at smaller w_o sizes, as is observed, because the internal water core is reducing in size.

We interpret these results to show that $[\text{Co}(\text{dipic})_2]^-$ resides in the water pool. Its location makes it accessible to direct collision with hexacyanoferrate(II) and electron transfer occurs. In contrast, when $[\text{Co}(\text{edta})]^-$ is present in the RM, no experimentally observable change in the OD stretch is found. The presence of $[\text{Co}(\text{edta})]^-$ does not significantly impact the H(D)-bonding or other water properties in the micellar water pool. This result is interpreted as this probe residing in the interfacial region, thereby making inaccessible for interaction with the hexacyanoferrate(II), hence shutting off electron transfer. These results do not rule out changes in the driving force for the reaction because of ion pairing with the sodium counterions for AOT. If this occurs, it might also affect the reaction rate by changing the redox potentials of the reactants.

In contrast to the $[\text{Co}(\text{edta})]^-/[\text{Fe}(\text{CN})_6]^{4-}$ reaction, which is shut off, the $[\text{Co}(\text{dipic})_2]^-/[\text{Fe}(\text{CN})_6]^{4-}$ reaction showed a small acceleration within the RM compared to the rate in aqueous media. Marcus theory⁵⁴ predicts that this may be due to three factors: (1) decreased inner-sphere reorganizational energies, (2) increased driving force for the reaction, for example, changes in the redox potentials of the oxidant/reductant, and (3) decreased outer-sphere reorganizational energies. The UV-vis, Supporting Information, Figure S1, and ¹H NMR spectral features are consistent with no major structural changes and no major difference in inner-sphere reorganizational energies is present. This leaves changes in the driving force of the reaction or the decreased outer-sphere reorganizational energies to account for the changes in the reaction rate. On the basis of reactant self-exchange rate constants and the overall thermodynamic driving force, the Marcus cross relationship can be used to calculate the outer-sphere electron transfer rate constant for each reaction condition.⁵⁵ It is well-known that the self-exchange rate for the $[\text{Fe}(\text{CN})_6]^{3-/4-}$ couple is counterion mediated.^{56,57} For the aqueous reaction, using a self-exchange rate constant for the $[\text{Co}(\text{dipic})_2]^{-/2-}$ couple of $0.4 \text{ M}^{-1} \text{ s}^{-1}$ and a reduction potential of 0.40 V (vs NHE),³² along with those for the $[\text{Fe}(\text{CN})_6]^{3-/4-}$ couple (estimated under the conditions here as $5 \times 10^3 \text{ M}^{-1} \text{ s}^{-1}$ ⁵⁷ and 0.41 V) the calculated rate constant for the $[\text{Co}(\text{dipic})_2]^-/[\text{Fe}(\text{CN})_6]^{4-}$ reaction is $\sim 45 \text{ M}^{-1} \text{ s}^{-1}$. This is in excellent agreement with the experimentally observed value in aqueous media of $55 \pm 10 \text{ M}^{-1} \text{ s}^{-1}$ supporting the outer-sphere nature of the reaction. Now that we have demonstrated the applicability of Marcus theory for this system, we can similarly apply the method to the RM environment.

Correa and co-workers,⁴² as well as Doherty and Charlton,⁴³ have reported that the redox potential for the $[\text{Fe}(\text{CN})_6]^{3-/4-}$ couple is not dramatically altered (more negative by 0.04 V) from its aqueous value when placed in the water pools confined within $w_o = 10$ RMs prepared using NaAOT/isooctane. Assuming that the reduction potential and self-exchange rate for the $[\text{Co}(\text{dipic})_2]^{-/2-}$ couple remains similarly unaltered and taking the redox potential for the $[\text{Fe}(\text{CN})_6]^{3-/4-}$ couple as 0.37 V and its self-exchange rate as $1 \times 10^{-4} \text{ M}^{-1} \text{ s}^{-1}$ ⁵⁷ to account for further catalysis by the Na^+ ions associated with the 0.2 M AOT surfactant, a cross reaction rate constant of $\sim 63 \text{ M}^{-1} \text{ s}^{-1}$ can be calculated for the $w_o = 10$ system. This calculated RM rate constant is 1.4 times higher than that calculated for the aqueous system. A similar rate enhancement is seen at $w_o = 10$. If we assume the driving force for the reduction of $[\text{Co}(\text{dipic})_2]^-$ by $[\text{Fe}(\text{CN})_6]^{4-}$ is little changed when confined within the RM, we can tentatively conclude that the small but significant rate acceleration seen for the reaction inside the RM is explained by

an increase in the self-exchange rate for the latter as a result of localized Na^+ mediation at the interfacial sites.

The observed increase in rate constant could also be due to changes in the nature of the water structure, ionic strength, and the dielectric constant at the RM interface.^{46,58,59} Since ionic strength will change as the size of the RM changes, the altered ionic composition at the interface will affect the rate constant. Although Debye-Hückel theory predicts a rate increase with increasing ionic strength⁶⁰ (decreasing w_o) this is not what is observed. Debye-Hückel theory can be used to “back calculate” the ionic strength in the interior of the RM assuming that the rate constant at zero ionic strength is equal to that determined in pure water. A simplified calculation using -4 and -1 for the charges on the reactants gives a back calculated ionic strength of $\sim 0.01 \text{ M}$ which is not reasonable for the interior of the RM since there is a 0.2 M Na^+ ionic strength contribution from the NaAOT surfactant itself. This suggests that the charges on the reactant ions must be lower than the -1 or -4 used in the calculations. This explanation is also consistent with the ¹H NMR and IR studies wherein it is proposed that $[\text{Co}(\text{edta})]^-$ resides in the interfacial region of the RM. Ion pairing, for example, $\{\text{Na}^+ / [\text{Co}(\text{edta})]^- \}^0$ would neutralize the charge thereby facilitating migration from the water pool into the interfacial region (Figure 1, regions B and C).

Considering that the two Co-complexes have similar redox potentials, the observed differences in interactions with the interface may be attributed to size and geometry. The smaller size of the $[\text{Co}(\text{edta})]^-$ would lead to a higher ion pairing constant and form a more compact object. Both factors may allow for easier penetration of the complex into the interface. The decreased rate constant observed at the smallest RM ($w_o = 7$) may reflect forced ion-pairing of $[\text{Co}(\text{dipic})_2]^-$ with Na^+ .

Studies of reactions in RMs must also consider size and occupancy restrictions in each nanostructure. In the concentration range used in the present kinetic study, it is estimated that on average there are 0.2 to 1.0 cobalt(III) complexes in a $w_o = 7$ RM and 1.5 to 7.6 cobalt(III) complexes in a $w_o = 20$ RM. Using an average radius of 4.5 \AA for the metal complexes and 35 \AA for the radius of a $w_o = 20$ RM, about 500 metal complexes can geometrically fit within such a RM whereas 19 metal complexes can fit within a $w_o = 5$ RM with a radius of 12 \AA .² Since the number of waters range from a few hundred to over 6000 between $w_o = 5$ and 20 ,⁶¹ the actual metal complex occupancy is significantly lower than geometrically possible, so ion-ion interactions will be much smaller even if the concentrations of Fe and Co complexes are comparable. While the decreasing statistical collision frequency explains the fall off in the rate of reduction of $[\text{Co}(\text{dipic})_2]^-$ at low w_o values, it cannot explain the complete suppression of the reduction of $[\text{Co}(\text{edta})]^-$ within the RM. The present study thus provides evidence that confinement of metal complexes within RMs affects reactivity based on location.

The question remains whether these observations are exclusively a matter of restricted collisions, or other factors such as solvation. A number of reported studies concerning the redox partners used here have described kinetic effects arising from the changing nature of solvation of the reactants.¹ For example, the observed rate constant for the outer-sphere reduction of $[\text{Co}(\text{NH}_3)_4(\text{C}_2\text{O}_4)]^+$ by hexacyanoferrate(II) at $20 \text{ }^\circ\text{C}$ showed a 3-fold increase as the methanol content in methanol/water mixtures was increased from 5% to 30%.¹ These effects were rationalized by preferential solvation effects on the outer-sphere complex and its dissociation products. A small increase ($\sim 25\%$)

in the observed rate of reduction of $[\text{Co}(\text{edta})]^-$ by $[\text{Ru}(\text{NH}_3)_5\text{py}]^{2+}$ (py = pyridine) was similarly observed in 36.2% methanol/water compared to pure aqueous solution. By measuring the changes to the redox potential of the $[\text{Co}(\text{edta})]^-/2-$ couple and the equilibrium constant of the outer-sphere complex in the different media, the result was a small decrease in the electron transfer rate. This was rationalized in terms of an extra component ($\sim 7.6 \text{ kJ mol}^{-1}$) to the reorganization energy that is not present in neat solvent.² Thus, although the current study has focused on location, the solvation of these Co(III) complexes are very much impacted by their location and could contribute to some of the observed differences.

Confinement effects in RMs leading to significant changes in kinetic and equilibration behavior have been reported in other studies of complex ion reactions. For example, Crans and Johnson observed a 3-fold decrease in the equilibrium constant for 1:1 complexation of ascorbic acid with $\text{VO}_2^+(\text{aq})$ upon inclusion within $\text{H}_2\text{O}/\text{NaAOT}/\text{isooctane}$ RMs compared to bulk aqueous media.^{53,62} In contrast, the subsequent intramolecular electron transfer process within the VO_2^+ -ascorbate complex to give $\text{VO}^{2+}(\text{aq})$ and ascorbate radical was increased 2-fold inside the micelle.⁶² The overall change in reactivity was ascribed to relocation of ascorbic acid from an aqueous environment into the interface region of the RM. Assignment of location was based on 1-D and 2-D NMR as well as electron paramagnetic resonance (EPR) spectroscopic studies.⁵³ These findings along with those reported here indicate that the rate constants for complexation and electron transfer reactions are affected by changes to their local environment. Importantly, the present studies show that when significant compartmentalization of reactants occurs, for example, the case of reduction of $[\text{Co}(\text{edta})]^-$ by $[\text{Fe}(\text{CN})_6]^{4-}$ in a RM microemulsion, a reaction can be switched off altogether.

CONCLUSION

The rates of outer-sphere reaction between two redox active cobalt(III) complexes and hexacyanoferrate(II) are strongly affected by environment. The incorporation of cobalt(III) complexes into the nonconventional aqueous medium present in confined water pools within RMs leads to very different redox behavior for two complexes with very similar redox potentials. The reductant used for both cobalt(III) complexes, the highly negatively -4 charged hexacyanoferrate(II), is presumed to be located within the water pool (Figure 1 location A) as has been previously described.⁴² Thus, when the cobalt(III) reactant; $[\text{Co}(\text{dipic})_2]^-$, is also located in, or accessible to, the water pool (Figure 1 location A), its reduction is moderately accelerated because the reactants are available for reaction in the same compartment. In contrast, the cobalt(III) reactant, $[\text{Co}(\text{edta})]^-$, is located in a region of the interface inaccessible to the core water pool and presumably at least partially penetrated into the interfacial layer (Figure 1 location B or C). As a consequence, the redox partners are now located in different compartments, and the corresponding reaction is completely switched off as a result of separation. Alternatively, the shut down of the reaction may also be due to changes in the driving force for the reactions as a result of ion pairing with Na^+ ions in the RM interior. The ^1H NMR data is consistent with $[\text{Co}(\text{dipic})_2]^-$ being less associated with the interface than the $[\text{Co}(\text{edta})]^-$ complex. The IR studies indicate an environment for the $[\text{Co}(\text{dipic})_2]^-$ complex either in or accessible to the core water pool but an alternative environment for the $[\text{Co}(\text{edta})]^-$ complex somewhat removed from the water pool. In summary,

this study shows that confinement (compartmentalization) of reactants in a dynamic reverse micellar system can significantly impact reactivity and in some cases switch off reaction altogether.

ASSOCIATED CONTENT

Supporting Information

Further details are given in Figure S1. This material is available free of charge via the Internet at <http://pubs.acs.org>.

AUTHOR INFORMATION

Corresponding Author

*E-mail johnson@mnsu.edu (M.D.J.), crans@lamar.colostate.edu (D.C.C.).

ACKNOWLEDGMENTS

M.D.J., and D.C.C. thank NSF for funding this research (CHE 0628260). Christopher D. Rithner (CSU) is thanked for help in recording and interpreting the NMR spectra. Finally, the Pacific Northwest National Laboratory (PNNL) is thanked for the use of their NMR instruments. We also acknowledge the reviewers for this manuscript and their insightful comments that helped our interpretation of the results.

REFERENCES

- (1) Anbalagan, K.; Geethalakshmi, T.; Poonkodi, S. P. *R. J. Phys. Chem.* **2003**, *107*, 1918–1927.
- (2) Villa, I.; Sanchez, F.; Perez-Tejeda, P. *Int. J. Chem. Kinet.* **2009**, *41*, 658–666.
- (3) Maitra, A. *J. Phys. Chem.* **1984**, *88*, 5122–5125.
- (4) Levinger, N. E. *Science* **2002**, *298*, 1722–1723.
- (5) Park, S.; Moilanen, D. E.; Fayer, M. D. *J. Phys. Chem. B.* **2008**, *112*, 5279–5290.
- (6) Lesh, F. D.; Allard, M. M.; Shanmugam, R.; Hryhorczuk, L. M.; Endicott, J. F.; Schlegel, H. B.; Verani, C. N. *Inorg. Chem.* **2011**, *50*, 969–977.
- (7) Bakac, A. Chemical kinetics as a mechanistic tool. In *Physical Inorganic Chemistry: Principles, Methods, and Models*; Bakac, A., Ed.; John Wiley: New York, 2010; pp 367–424.
- (8) Binks, D. A.; Spencer, N.; Wilkie, J.; Britton, M. M. *J. Phys. Chem. B* **2010**, *114*, 12558–12564.
- (9) Lucio, M.; Lima, J. L. F. C.; Reis, S. *Curr. Med. Chem.* **2010**, *17*, 1795–1809.
- (10) Yang, L.; Crans, D. C.; Miller, S. M.; La Cour, A.; Anderson, O. P.; Kaszynski, P. M.; Godzala, M. E.; Austin, L. D.; Willsky, G. R. *Inorg. Chem.* **2002**, *41*, 4859–4871.
- (11) Crans, D. C. *J. Inorg. Biochem.* **2000**, *80*, 123–131.
- (12) Crans, D. C.; Trujillo, A. M.; Pharazyn, P. S.; Cohen, M. D. *Coord. Chem. Rev.* **2011**, *255*, 2178–2192.
- (13) Ogino, H.; Ogino, K. *Inorg. Chem.* **1983**, *22*, 2208–2211.
- (14) Xue, Y.; Traina, S. J. *Environ. Sci. Technol.* **1996**, *30*, 1975–1981.
- (15) Chowdhury, P. K.; Ashby, K. D.; Dutta, A.; Petrich, J. W. *Photochem. Photobiol.* **2000**, *72*, 612–618.
- (16) De Marco, A.; Menegatti, E.; Luisi, P. L. *J. Biochem. Biophys. Methods* **1986**, *12*, 325–333.
- (17) Evans, R.; Timmel, C. R.; Hore, P. J.; Britton, M. M. *Chem. Phys. Lett.* **2004**, *397*, 67–72.
- (18) Evans, S. E.; Grigoryan, A.; Szalai, V. A. *Inorg. Chem.* **2007**, *46*, 8349–8361.
- (19) Evans, S. E.; Mon, S.; Singh, R.; Ryzhkov, L. R.; Szalai, V. A. *Inorg. Chem.* **2006**, *45*, 3124–3138.
- (20) Fletcher, P. D. I.; Howe, A. M.; Robinson, B. H. *J. Chem. Soc., Faraday Trans.* **1987**, *83*, 985–1006.
- (21) Fletcher, P. D. I.; Steyler, D. C.; Tack, R. D. *J. Chem. Soc., Faraday Trans.* **1979**, *75*, 481–496.

- (22) Bru, R.; Sanchez-Ferrer, A.; Garcia-Carmona, F. *Biochem. J.* **1995**, *310*, 721–739.
- (23) Pietrini, A. V.; Luisi, P. L. *Biochim. Biophys. Acta* **2002**, *1562*, 57–62.
- (24) Luisi, P. L.; Giomini, M.; Pileni, M. P.; Robinson, B. H. *Biochem. Biophys. Acta* **1988**, *947*, 209–246.
- (25) Osfouri, S.; Stano, P.; Luisi, P. L. *J. Phys. Chem. B* **2005**, *109*, 19929–19935.
- (26) Chakraborty, A.; Seth, D.; Chakrabarty, D.; Hazra, P.; Sarkar, N. *Chem. Phys. Lett.* **2005**, *405*, 18–25.
- (27) Kumbhakar, M.; Nath, S.; Sarka, S. K.; Mukherjee, A. T.; Pal, H. *J. Chem. Phys.* **2005**, *123*, 034705/1–034705/11.
- (28) Dutta Choudhury, S.; Kumbhakar, M.; Nath, S.; Sarka, S. K.; Mukherjee, A. T.; Pal, H. *J. Phys. Chem. B* **2007**, *111*, 8842–8845.
- (29) Zaslavskaya, L. A.; Polyakova, I. N.; Rybakov, V. B.; Polynova, T. N.; Poznyak, A. L.; Sergienko, V. S. *Crystallogr. Rep.* **2006**, *51*, 448–458.
- (30) Zhou, K.; Li, J.; Zhang, Y.; Fang, J.; Chen, Z. *Jiegou Huaxue* **1985**, *4*, 218–20.
- (31) Das, B.; Ghosh, K.; Baruah, J. B. *J. Coord. Chem.* **2011**, *64*, 583–589.
- (32) Mauk, A. G.; Coyle, C. L.; Bordignon, E.; Gray, H. B. *J. Am. Chem. Soc.* **1979**, *101*, 5054–5056.
- (33) Davies, K. M.; Hussam, A.; Rector, B. R. Jr.; Owen, I. M.; King, P. *Inorg. Chem.* **1994**, *33*, 1741–1747.
- (34) Rosenhein, L.; Speiser, D.; Haim, A. *Inorg. Chem.* **1974**, *13*, 1571–1575.
- (35) Mauk, A. G.; Bordignon, E.; Gray, H. B. *J. Am. Chem. Soc.* **1982**, *104*, 7654–7657.
- (36) Stadler, C. C.; Franco, C. V.; Neves, A. *J. Braz. Chem. Soc.* **1991**, *2*, 31–36.
- (37) Ogino, H.; Kikkawa, E.; Shimura, M.; Tanaka, N. *Dalton Trans.* **1981**, *3*, 894–896.
- (38) Lin, L.-M.; Huang, J.-C.; Huang, D.-L.; Yeh, A. *J. Chin. Chem. Soc.* **2005**, *52*, 455–462.
- (39) Lin, C. S.; Chien, C. F.; Yeh, A. *J. Chin. Chem. Soc.* **1991**, *38*, 217–220.
- (40) Sun, P.; Li, F.; Chen, Y.; Zhang, M.; Zhang, Z.; Gao, Z.; Shao, Y. *J. Am. Chem. Soc.* **2003**, *125*, 9600–9601.
- (41) Garcia-Fernandez, E.; Prado-Gotor, R.; Sanchez, F. *J. Phys. Chem. B* **2005**, *109*, 15087–15092.
- (42) Molina, P. G.; Silver, J. J.; Correa, N. M.; Sereno, L. *J. Phys. Chem. C* **2007**, *111*, 4269–4276.
- (43) Charlton, I. D.; Doherty, A. P. *Electrochem. Commun.* **1999**, *1*, 176–179.
- (44) Stahla, M. L.; Baruah, B.; James, D. M.; Johnson, M. D.; Levinger, N. E.; Crans, D. C. *Langmuir* **2008**, *24*, 6027–6035.
- (45) Dwyer, F. P.; Gyarfás, F. C.; Mellor, D. P. *J. Phys. Chem.* **1955**, *59*, 296–297.
- (46) Crans, D. C.; Rithner, C. D.; Baruah, B.; Gourley, B. L.; Levinger, N. *J. Am. Chem. Soc.* **2006**, *128*, 4437–4445.
- (47) (a) The λ_{max} of 538 nm is consistent with values reported for hexadentate [Co(edta)][−] (535 nm): Osvath, P.; Lappin, A. G. *Inorg. Chem.* **1987**, *26*, 195–202. [Co(edtaH)(H₂O)] with one arm dissociated has a reported λ_{max} at 551 nm: Shimi, I. A. W.; Higginson, W. C. *J. Chem. Soc.* **1958**, 260. (b) Jolley, W.; Stranks, D. R.; Swaddle, T. *W. Inorg. Chem.* **1992**, *31*, 507–511.
- (48) Rosokha, S. V.; Kochi, J. K. *Acc. Chem. Res.* **2008**, *41*, 641–653.
- (49) Bain, A. D.; Rex, D. M.; Smith, R. N. *Magn. Reson. Chem.* **2001**, *39*, 122–126.
- (50) Wand, A. J.; Ehrhardt, M. R.; Flynn, P. F. *Proc. Natl. Acad. Sci. U.S.A.* **1998**, *95*, 15303–15308.
- (51) Piletic, I. R.; Moilanen, D. E.; Spry, D. B.; Levinger, N. E.; Fayer, M. D. *J. Phys. Chem. A* **2006**, *110*, 4985–4999.
- (52) Baruah, B.; Swafford, L. A.; Crans, D. C.; Levinger, N. E. *J. Phys. Chem. B* **2008**, *112*, 10158–10164.
- (53) Fenn, E. E.; Moilanen, D. E.; Levinger, N. E.; Fayer, M. D. *J. Am. Chem. Soc.* **2009**, *131*, 5530–5539.
- (54) Brunschwig, B. S.; Ehrenson, S.; Sutin, N. *J. Phys. Chem.* **1986**, *90*, 3657–3668.
- (55) Marcus, R. A. *J. Chem. Phys.* **1956**, *24*, 966–978.
- (56) Takagi, H.; Swaddle, T. W. *Inorg. Chem.* **1992**, *31*, 4669–4673.
- (57) Fu, Y.; Cole, A. S.; Swaddle, T. W. *J. Am. Chem. Soc.* **1999**, *121*, 10410–10415.
- (58) Baruah, B.; Roden, J. M.; Sedgwick, M.; Correa, N. M.; Crans, D. C.; Levinger, N. E. *J. Am. Chem. Soc.* **2006**, *128*, 12758–12765.
- (59) Fletcher, P. D. I. *J. Chem. Soc., Faraday Trans.* **1987**, *83*, 1493–1506.
- (60) Wilkins, R. G. *Kinetics and Mechanisms of Reactions of Transition Metal Complexes*, 2nd ed.; Wiley-VCH: New York, 1991.
- (61) De, T. K.; Maitra, A. *Adv. Colloid Interface Sci.* **1995**, *59*, 95–99.
- (62) Crans, D. C.; Baruah, B.; Gaidamauskas, E.; Lemons, B. G.; Lorenz, B. B.; Johnson, M. D. *J. Inorg. Biochem.* **2008**, *102*, 1334–1347.
- (63) Wilkins, P. C.; Johnson, M. D.; Holder, A. A.; Crans, D. C. *Inorg. Chem.* **2006**, *45*, 1471–1479.
- (64) Gazzaz, H. A.; Ember, E.; Zahl, A.; van Eldik, R. *Dalton Trans.* **2009**, 9486–9495.